Forces in Mechanics 18 (2025) 100302

Contents lists available at ScienceDirect

Forces in Mechanics

journal homepage: www.sciencedirect.com/journal/forces-in-mechanics

Enhancing repair of cracked plate using fiber-reinforced composite patch: Experimental and simulation analysis

Abdul Aabid [a,*], Muhammad Nur Syafiq Bin Rosli [b], Meftah Hrairi [b,*], Muneer Baig [a]

[a] Department of Engineering Management, College of Engineering, Prince Sultan University, PO BOX 66833, Riyadh 11586, Saudi Arabia
[b] Department of Mechanical and Aerospace Engineering, Faculty of Engineering, International Islamic University 53100 Kuala Lumpur, Malaysia

ARTICLE INFO

Keywords:
Stress intensity factor
Numerical simulation
Composite patch
Aluminium plate
And repair method

ABSTRACT

In this study, a fiber-reinforced composite patch was bonded to one side of a cracked aluminum plate using Araldite-2014 adhesive. Experimental tensile tests were conducted on both repaired and unrepaired plates, with further analysis of the effects of patch material and dimensions performed using ANSYS simulations. The effectiveness of the patch repair was evaluated through the stress intensity factor (SIF), as obtained from both experimental and finite element methods. To optimize patch parameters—such as material, thickness, width, and height design of experiments (DOE) approach was applied. Results indicate that the use of fiber-reinforced composite patches is an effective technique for repairing cracked aluminum structures, as it significantly reduces SIF. The findings suggest that repair efficiency can be further enhanced by carefully considering key factors such as patch dimensions, adhesive thickness, and crack length.

1. Introduction

The current method of repairing aircraft structure is by the mechanical repaired method. This method requires bolts, nuts, and screws as part of the repair and repairing with this technique may cause failure due to increment in the holes. The stress distribution is not even and concentrated on the edge of the hole. Therefore, light-weight composite patches have been utilized to stop the crack propagation of the aircraft structure. Generally, the properties of composite that have high specific stiffness and strength drive the method of reinforcing cracked structure. Thus, further research on composite patch is required to fully utilize and the advantages of using the composite patch in repairing thin-walled aircraft structure.

The design of aircraft, aerospace, and civil structures with damage-tolerant and fail-safe features necessitates rigorous and routine inspections to monitor defects [9]. The operational costs associated with maintaining aging aircraft structures worldwide are significant, as these structures are continuously degrading over time. To manage this degradation, regular and costly inspections are conducted to mitigate the risk of structural failure [26]. The advancements in composite materials, known for their high strength-to-weight ratios, and improved adhesive technologies have enabled the bonding of reinforcing patches to aircraft structures. The primary objective of such repair strategies is to effectively transfer the load from the damaged structure to the reinforcement, thereby reducing the crack propagation potential [23].

Composite patches have proven to be a promising approach for reinforcing cracked structures owing to the composite materials exceptional stiffness and strength in relation to its weight [32]. Bonded patch repair has many advantages over other traditional repairs like mechanically repair using different types of fasteners, rivets, and nuts that increase the stress concentration by adding more holes [24]. Bonded patch repair uses adhesive joints to connect the metal structure and patch surfaces. Adhesive joints have become widely used due to their ability to evenly distribute stress, enhancing the structure's resistance to damage [10,22,25]. Bonded assemblies facilitate a gradual transfer of load between components, mitigating stress concentration [17]. Despite the advantages of adhesive joints, a key drawback is the high stress concentration at the bond's termination point, often causing joint failure. To enhance the joint's overall strength and performance, it is necessary to minimize stress concentration within the adhesive layer [14]. Calculation of stress intensity factor (SIF) has been done by many researchers at the crack tip of repaired aircraft components [13].

Both experimental and analytical approaches done on a bonded composite patch in the existing work. Parameters that they must investigate include the geometry of the patch, length of the patch, thickness of the patch, type of adhesive use, effect of incline crack, and

* Corresponding authors.
E-mail addresses: aaabid@psu.edu.sa (A. Aabid), meftah@iium.edu.my (M. Hrairi).

https://doi.org/10.1016/j.finmec.2024.100302
Received 15 September 2024; Received in revised form 18 November 2024; Accepted 13 December 2024
Available online 17 December 2024

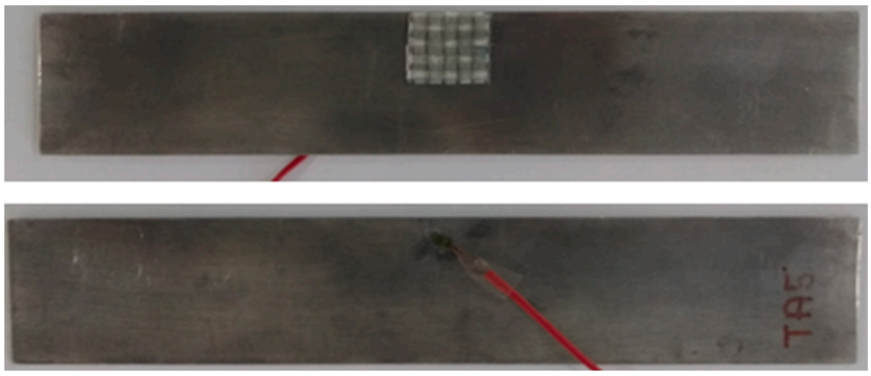

Fig. 1. Edge crack plate integrated with glass/epoxy patch.

stress intensity factor on the efficiency of the technique of repair. The different experiments might have different materials they used for the plate, patch, and adhesive, but some of them have the same types of specimens — some of the experiments used aluminium as their plate such as AA1035 [19], 20,024-T3 plates [28] and 7075-T6 [8].

The finite element (FE) analysis used to model cracked plate with composite patch under two different loading conditions [24]. In recent study, ANSYS used to obtain the results of SIF for repaired and unrepaired AL2024-T3 specimens [3,4]. The data optimization technique plays key role on determining optimum output in any field of engineering and sciences [21] also in bonded repair [34]. The advantage using DOE is energy saving and cost efficient approach [1,6] and high accuracy in results [11]. Some of other considered the parameters such as effect of patch lay-up sequence and the pre-crack angle on fatigue life [27]. Patched and unpatched parameters [13], focus with patch thickness effect [13], temperature and effect of humidity [30] for optimum of output.

The efficiency of composite patch repairs has been demonstrated across various configurations, materials, and loading conditions. Previous studies, such as that by Kaddouri et al., [18], have analyzed the impact of composite patch modifications, specifically through thickness adjustments, on the J Integral in repaired plates, highlighting the critical role of patch dimensions and bonding integrity in stress mitigation. Furthermore, Madani et al., [20] examined stress distribution in aluminum plates with a circular notch, repaired using graphite/epoxy composite patches, providing foundational insights into the role of patch materials in minimizing stress concentrations. Djebbar et al., [15] further expanded on this by employing cohesive zone modelling (CZM) and extended finite element methods (XFEM) to assess patch shapes and their effects on the performance of reinforced aluminum structures. Such analyses underscore the necessity of considering both patch geometry and the mechanical properties of composite materials in enhancing repair outcomes.

Recent advancements also explore the influence of patch bevelling, as seen in the work by Belhoucine and Madani, [12], who demonstrated that bevelled edges in composite patches can significantly reduce stress in damaged areas. Additionally, the performance of carbon fiber patches in elevating the failure strength of repaired plates is another area of growing interest, with studies indicating that carbon fibers can substantially improve durability and load-bearing capacity [31].

Current literature reveals that various methodologies have been employed to demonstrate bonded composite repairs. Furthermore, significant research has been conducted on the mitigation of SIF by adjusting model parameters. Recently, the DOE approach has been utilized to explore these parameters with substantial data, leading to more accurate SIF mitigation insights. This study primarily focuses on applying the DOE approach to investigate current work model parameters that are underrepresented in the existing literature. The objective is to analyse the effectiveness of fiber-reinforced composites for bonded composite patch repairs on thin plates. Experimental work has been carried out to validate the simulation model. Upon achieving satisfactory results, additional simulations were performed to generate data for DOE analysis, specifically to examine SIF for both unrepaired and repaired edge-cracked plate structures.

Table 1
Material properties of fiberglass and epoxy resin.

Material	Young's Modulus $\mathbf{E_1 = E_2}$ (GPa)	Shear modulus **G** (GPa)	Density $\boldsymbol{\rho}$ ($\mathbf{g/cm^3}$)	Poisson ratio υ
Woven fiberglass	71	30	2.55	0.22
Epoxy resin	3.5	1.25	1.2	0.33

2. Experimental work

2.1. Specimen preparation

While aluminum 2024-T3 with dimensions 200×40 mm and a 1 mm thickness is commonly employed in similar studies ([18]; Madani et al., 2010), this study used aluminum 1100 with slightly modified dimensions of 150×38 mm and a thickness of 1 mm due to material availability and equipment constraints. This adjustment did not alter the scope or objectives of the study and allowed for meaningful comparisons with established literature.

To prepare the sample of experiment for the current work the Aluminium-1100 alloy specimen cut through the sheet metal cutter with the dimension of 150 mm hight and 38 mm of width and the thickness of 1 mm. Later, the plates were cleaned via metal cleaner in order to remove the rough surface and unwanted particles/meshes. Then, the crack on specimens has been prepared by using a micro electrical discharge machine (Micro-EDM) to have crack with the length of 7.33 mm and 0.06 mm width. The width of the crack has been generated with maximum possibility of Micro-EDM machine that available in IIUM laboratory which is 600 μm. After successfully created the crack the length of crack on the specimen was measured using a digital Nikon microscope [7] with support of graphical scale.

The process includes a tensile test of the patch, finding the location of the strain gauge, and the tensile test of the integrated specimen. Tensile tests were carried out on a universal INSTRON machine. The purpose of the tests was to obtain the properties of the patch and strain value on the repaired specimen to get SIF.

Strain measurements were conducted on the loaded specimen to measure the SIF, strain measurements on the loaded specimens have been carried out using the electrical resistance strain gages of type KFG-

Table 2
Glass/epoxy patch properties.

Material	E_1	E_2	E_3	v_{12}	v_{23}	v_{31}	G_{12}	G_{23}	G_{31}
Glass/Epoxy	16.6 GPa	16.6 GPa	3.57 GPa	0.3	0.3	0.35	5.2	5.2	1.32

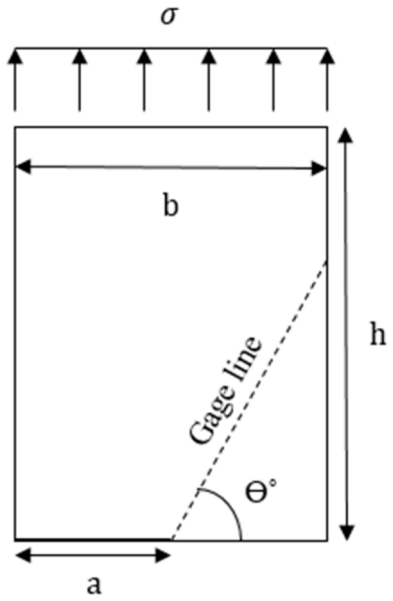

Fig. 2. Solution domain for the edge cracked plate.

1–120-C1 (the length of the gage is 1 mm) and made by KYOWA Japan. The strain gauge wire was secured with tape to provide strain relief. Fig. 1 illustrates both the front and back of the integrated specimen.

2.2. Patch preparation

The selection of material for the patch is based on the existing study [9] which recommended composite patch bonded with the adhesive produced very efficient repairs, with high levels of retardation and low rates of crack growth. Therefore, the current work prepared the sample of patch using the woven fiberglass and porous materials such as mylar, peel ply, release film, and bleeder are cut according to the size of the mold used (250 mm by 370 mm). For resin, epoxy resin is used in this experiment with a ratio of 2 resin to 1 hardener. With a 15 percent volume fraction of fiber and 85 percent of the resin, the weight of resin can be calculated using Eq. (2).

$$\frac{V_f}{V_r} = \frac{W_f/\rho_f}{W_r/\rho_r} \tag{1}$$

$$W_r = \frac{\rho_r}{\frac{V_f}{V_r} \times \frac{\rho_f}{W_f}} \tag{2}$$

Where W_f = weight of fiberglass, ρ_f = density of fiberglass and ρ_r = density of resin.

The current experimental utilized the woven fiberglass which having 0-degree, and 90-degree orientation and aim is to minimize the thickness as much as possible which should be less than the host thickness. The properties of both fiberglass and epoxy resin are specified in Table 1.

The technique used to fabricate the single-layer composite patch is by using a vacuum bagging process. In this procedure, the patches are cured for 2 h using a pump machine. Then, the composite was left for 24 h to cure thoroughly in normal temperature. Since the mold having the large diameter, cut patch from the center of the mold to get accuracy in the thickness and the final thickness of the patches is 0.6 mm. Later on, the patch sheet cut into square of 20 mm x 20 mm to used as repair materials for host plate. The purpose of this research is to study the effect of unpatched and patched with different thicknesses on the SIF from the repair. The tensile test was done on the fabricated glass/epoxy composite plate to obtain the mechanical properties of the patch specimen in Table 2.

2.3. Determination of strain gauge location

Before applying strain gauge onto the cracked specimen, the location of the strain gauge is determined by using Dally and Sanford strain gauge technique [29]. This technique is required to find the maximum radial location, r max of a strain gauge that is 60° from the crack tip. To determine the r max value, mesh analysis was done in ANSYS with the model shown in Fig. 2.

The strain gauge was attached between the range of maximum and minimum radial location using multipurpose glue. In this experiment, the location of the strain gauge was glued at 0.5 mm away from the crack tip. Based on the theory used by Dally and Sanford, a graph of ln (ε) vs. ln (r) is plotted, which show linear and nonlinear portion, as shown in Fig. 3. The point where it diverged gives ln (r max) value. For minimum radius, r minimum the value is 0.05 mm from the crack tip.

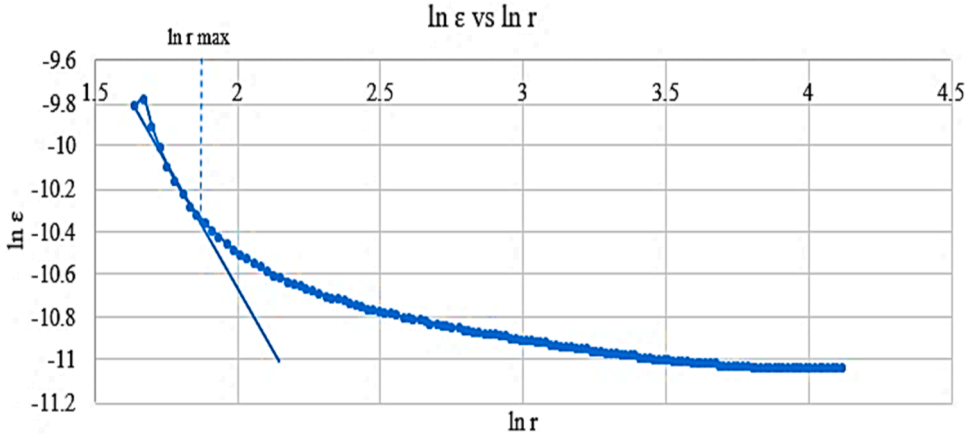

Fig. 3. Graph of ln ε vs. ln r.

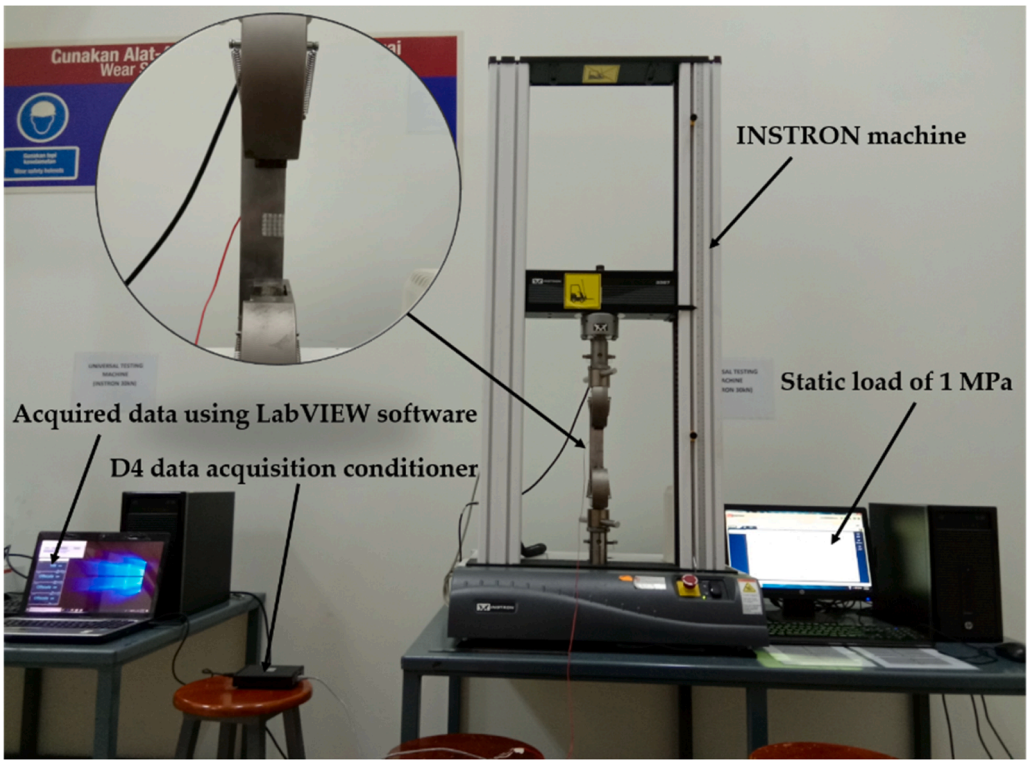

Fig. 4. Experimental setup.

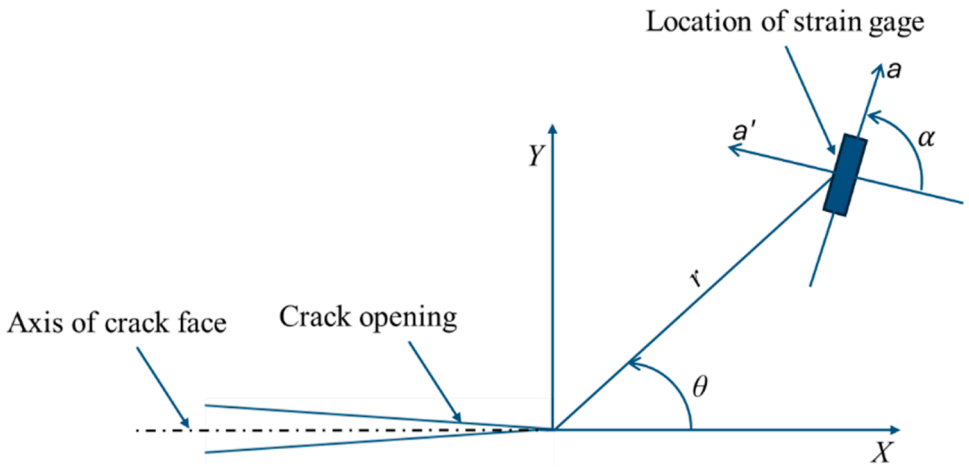

Fig. 5. DS technique for strain gage location.

2.4. Experimental procedure

To make a perfect bond between the host plate and composite repair patch used Araldite-2014 adhesive bond. Prior to bonding, the aluminum plates were prepared by cleaning the surfaces with a metal cleaner to remove any contaminants that could affect adhesion. Next, the composite patch and aluminum plate surfaces were lightly sanded to promote mechanical interlocking and ensure strong adhesive bonding. After surface preparation, the Araldite-2014 adhesive was applied uniformly to the bonding area of the aluminum plate with the thickness of 0.03 mm. The composite patch was then carefully placed onto the adhesive layer, ensuring even contact and alignment with the aluminum surface. Pressure was applied uniformly to the bonded assembly using a clamping mechanism to achieve consistent adhesive thickness and prevent air bubbles. The assembly was left to cure at room temperature for 24 h, as recommended by the adhesive manufacturer. After curing, visual inspections were performed to verify adhesive coverage and bonding integrity.

In this study, a uniaxial tensile load of 1 MPa was applied to evaluate the initial efficiency of the composite patch in mitigating stress on a damaged aluminum plate. The choice of a lower load enabled precise measurements of the SIF and helped establish baseline data without the influence of high-load variability. Future studies may explore the patch performance under increased loads to assess its efficiency in more

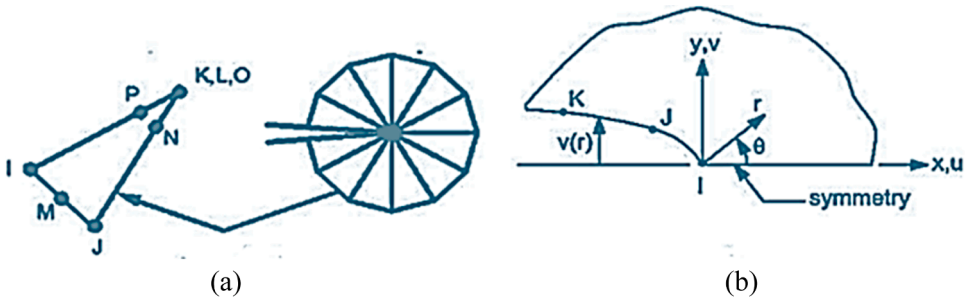

Fig. 6. the singular elements used in the finite element model: (a) the special element near the crack tip, and (b) the nodes around the crack tip that were used to calculate the displacement field.

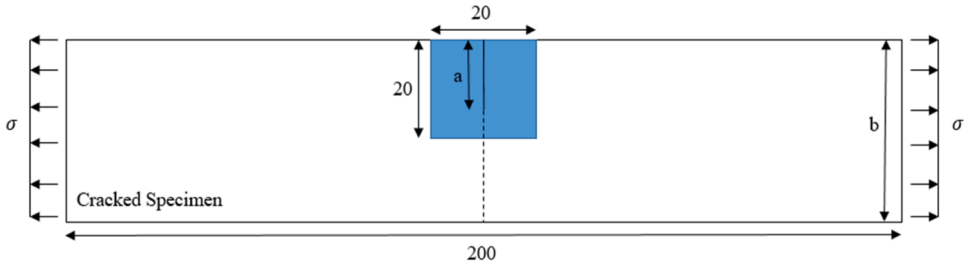

Fig. 7. Geometrical model of the patched specimen.

Table 3
Material Properties of Raw materials, Aluminium, Adhesive.

Material	Young's Modulus $\mathbf{E_1 = E_2}$	Shear modulus **G**	Density ρ	Poisson ratio υ
Aluminium	68.95	24	2.7	0.345
Araldite 2014	3.1	1.2	–	–
Units	GPa	GPa	g/cm^3	

demanding stress conditions. The experimental setup for investigating the bonded composite repair process is comprehensively illustrated in Fig. 4, which includes detailed views of both the front and rear sides of the aluminum plate with edge cracks. To conduct the tests, the aluminum specimen was firmly secured to the INSTRON machine using specialized grips, ensuring stability throughout the experimental procedure. The displacement control of the machine was set to a crosshead rate of 0.5 mm/min to regulate the movement accurately.

To ensure the repeatability and reliability of the results, each test was performed five times, and the average values were calculated to provide a consistent dataset. This approach allowed for a thorough evaluation of the experimental outcomes and helped to mitigate any potential discrepancies in the measurements. Attention to detail was paramount in the installation of strain gauges on the test specimens. Each gauge was meticulously applied to ensure strong, defect-free adhesion. The orientation and radial position of the strain gauges were carefully monitored during installation, and a magnifying lens was used to confirm the correct alignment and placement of each gauge. This precision was essential for obtaining accurate strain measurements.

Strain data was acquired using the Micro-Measurements model D4 Data Acquisition Conditioner, which provided detailed and precise readings of the strain experienced by the specimen. The collected data was then stored and analyzed using LabView software, facilitating a comprehensive examination of the experimental results. For the strain gauge measurements, quarter bridge configurations were employed, which are known for their accuracy and reliability in measuring strain.

2.4.1. *Measurement of SIF*

The single strain gage (DS) technique, introduced by Dally and Sanford in 1987, was employed to calculate the Mode I SIF. This method has been both theoretically and experimentally validated by [29] for accurate SIF determination. The DS technique relies on the precise location of a strain gage relative to the crack tip, defined by radial (r) and angular (θ) coordinates as shown in Fig. 5.

Sarangi et al., [29] proposed an equation for calculating the Mode I SIF in plane stress experimental fracture conditions.

$$2G\varepsilon_{aa} = \frac{1}{\sqrt{r}}\left[\frac{K_{1(total)}}{\sqrt{2\pi}}\left(k\cos\frac{\theta}{2} - \frac{1}{2}\sin\theta\sin\frac{3\theta}{2}\cos 2\alpha + \frac{1}{2}\sin\theta\cos\frac{3\theta}{2}\sin 2\alpha\right)\right] \tag{3}$$

$$k = \frac{1-\upsilon}{1+\upsilon} \tag{4}$$

Where, G represents the shear modulus and k the bulk modulus of the material. The term ε denotes the measured strain along the radial direction, r is the radial distance from the crack tip to the strain gage, θ is the angular position, and α is the strain gage orientation. The strain data obtained from the gage was used to compute the total SIF through Eq. (4).

3. Finite element model

Further research has been conducted through the FE methodology using the latest version of Ansys 2024 R2 software. The advantage of this technique can conduct numerical simulations for different variables of the problem definition. For the experimental work only one sample has been prepared and determined the SIF to validate the current FE work.

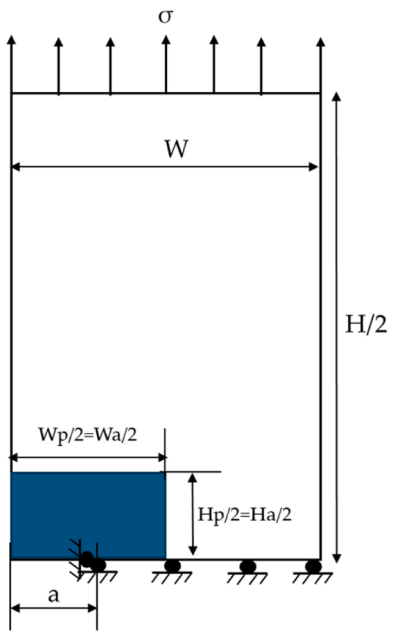

Fig. 8. Half-model of the plate.

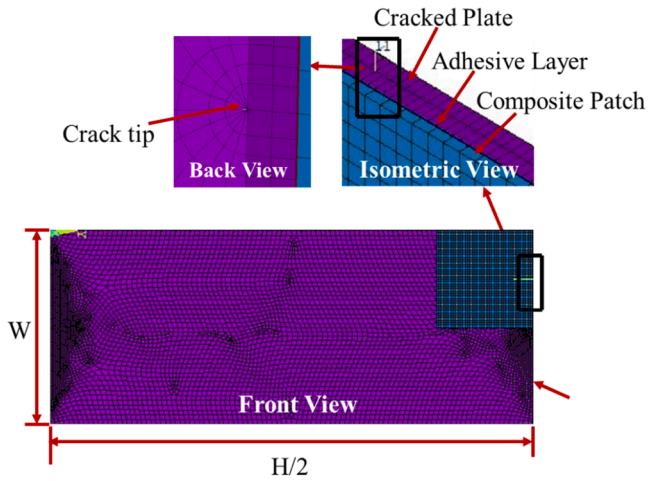

Fig. 9. Mesh model.

Once the validation has been done further changes has been made in the FE model to extract more results.

Because the stress and strain near the crack tip change rapidly, we used singular elements to accurately represent the behavior of the crack [5]. These elements have special nodes around the crack tip that help us calculate the displacement field needed for the SIF equation. Fig. 6(a) shows the singular elements used, and Fig. 6(b) illustrates the nodes around the crack tip that were used for the displacement calculations.

Used ANSYS FE analysis to calculate the SIF with good accuracy. Obtained the displacement near the crack tip from the FE analysis and used it in Eq. (5) to calculate the SIF.

$$K_I = \sqrt{2\pi}\,\frac{2\mu A}{1+k} \tag{5}$$

3.1. Geometry and modelling

As mentioned in the Section 2.1 the aluminum 2024-T3 has been found extensively in the literature therefore to continue this phenomenon FE method has been used (Fig. 7). Later, the parameters and dimensions has been varied for plate, patch and adhesive for optimization work. Here, the rectangular shape of repaired patch with the dimensions of 20 mm square and the thickness of 0.5 mm were considered. The adhesive bond for the current work considered used araldite 2014 [2]. Same as the experimental work, 1 MPa load has been applied to a bonded composite plate. Table 3 illustrates the mechanical properties of the aluminium plate, and adhesive bond.

Table 4
Mesh sensitivity analysis.

Mesh Type	No. of Elements	CPU Runtime (secs)	SIF (MPa$\sqrt{m}$)
Coarse	11,304	348	0.072
Intermediate	35,378	596	0.066
Fine	65,114	1197	0.065

3.2. Meshing and boundary conditions

For the integrated structure, three-dimensional ANSYS element SOLID186 is used to model the rectangular plate, adhesive layer, and composite material patch. SOLID186 element type contains 5-degrees 20-noded element.

Appropriate boundary conditions applied to an edge cracked plate which is shown in Fig. 8. At the crack tip regions, very fine mesh is generated to obtain a good result. Between the edge-cracked plate and composite patch, there was no debonding. A singular element of radius $r = 10$ mm and crack length $a = 5$ mm were used in the present study, the composite patch was integrated on the cracked area, and the applied tensile stress was 1 MPa. The model was symmetrical; therefore, only half of the model is considered, which is shown in Figs. 9.

The bonding between the aluminum plate, adhesive layer, and composite patch was treated as a fully bonded interface, assuming perfect adhesion without slippage or debonding under applied loads. In the FE model, a 'bonded' contact and target type of element were applied at both the plate-adhesive and adhesive-patch interfaces to simulate ideal adhesion conditions. This assumption was made based on the uniform application of adhesive and controlled curing process, which minimized the likelihood of interface failure during testing. The adhesive layer was assumed to have a uniform thickness across the bonding interface, with even load transfer properties, allowing the bonded model to simulate stress distribution effectively.

3.3. Mesh sensitivity analysis

A mesh sensitivity analysis was performed using ANSYS to determine the optimal mesh configuration for accurate SIF calculation while balancing computational efficiency. Three mesh types—coarse, intermediate, and fine—were evaluated. As shown in Table 4, the intermediate mesh configuration with 35,378 elements yielded SIF values that closely paralleled those of the fine mesh, with minimal deviation. This configuration required approximately 50 % less computational time than the fine mesh, making it a pragmatic choice for this study. Consequently, the intermediate mesh was used for all simulations, ensuring accurate SIF determination without excessive computational resources.

4. Design of experiments

[2,33,34], have used the DOE method to optimize repair in aircraft structures using bonded composite patches with the determination of SIF. Similarly, the bonded composite repair with the determination of J integral has been studied well by Belhouari et al., [11] and Fekih et al., [16]. This study focused on a rectangular aluminum plate with a central crack, reinforced with a composite patch and subjected to uniform tensile loading, as depicted in Fig. 7. The perfectly bonded composite patch inhibits crack propagation near the high-stress region by introducing shear stresses. To optimize parameters influencing the SIF - a

Table 5
Composite materials properties.

Material	E_1 (GPa)	E_2 (GPa)	E_3 (GPa)	ν_{12}	ν_{23}	ν_{31}	G_{12} (GPa)	G_{23} (GPa)	G_{31} (GPa)	Density
Carbon/Epoxy	134	10.3	10.3	0.33	0.33	0.53	5.5	5.5	3.2	
Boron/Epoxy	200	19.6	19.6	0.3	0.28	0.28	7.2	5.5	5.5	2000

Table 6
Selected parameters and their levels.

Parameters	Level 1	Level 2	Level 3
Material Type	Glass/Epoxy (GE)	Carbon/Epoxy (CE)	Boron/Epoxy (BE)
Thickness	0.5	0.75	1.0
Width	10	15	20
Height	10	15	20

Table 7
L_9 orthogonal array with a response value of SIF.

Run	Coded Values				Parameters				SIF
	A	B	C	D	M	Tp	Wp	Hp	
1	1	1	1	1	GE	0.5	10	10	0.056237
2	1	2	2	2	GE	0.75	15	15	0.045948
3	1	3	3	3	GE	1.0	20	20	0.046679
4	2	1	2	3	CE	0.5	15	20	0.062848
5	2	2	3	1	CE	0.75	20	10	0.059918
6	2	3	1	2	CE	1.0	15	15	0.057211
7	3	1	3	2	BE	0.5	20	15	0.052739
8	3	2	1	3	BE	0.75	10	20	0.072376
9	3	3	2	1	BE	1.0	15	10	0.043916

complex function of multiple controllable variables - DOE was deemed the most appropriate method due to its efficiency in optimizing various factors to achieve optimal outcomes.

For this specific case, four factors were considered that affect the value of SIF: the composite material type (M), thickness (Tp), width (Wp), and Height (Hp) of composite patch respectively. The properties of each composite materials type are illustrated in Table 2 and 5.

The considered parameters are similar to the study of Fekih et al., [16] in addition to that composite materials has been considered and obtained the SIF. The L_9 orthogonal arrays of Taguchi design as highly fractionated factorial designs have been employed in the present study (Montgomery, 2013). Each value of factors called levels is shown in Table 6.

A total 9-degree of freedom (DF) is the most suitable orthogonal array (OA) for experimentation called L_9 array, and these values are selected in ascending order as illustrated in Table 7.

5. Results and discussion

In this section, validation and analysis of the results obtained from both simulation and experimental work were done to study the effects of the composite patch on repairing plate aircraft structure. In ANSYS simulation, the SIF values obtained were normalized to observe the trend line made from the graphs. The values were normalized by dividing the repaired SIF with unrepaired SIF.

5.1. Validation of simulation with experimental result

To validate the result, obtain from the experimental, comparison of outcome was made between numerical and experimental data. The simulation result was obtained from the ANSYS software. While, for the experimental, the strain measurement obtained were substituted in Eq. (3) to get the SIF value. For this purpose, the comparison was made for unrepaired and repaired edge crack specimens. The comparison is shown in Table 8. Since the percentage of error is <10 percent, the result obtained can be accepted. Furthermore, the reduction of SIF after repair shows that the simulation and experiment are both correct.

5.2. Calculation of normalized SIF

In this study, the primary focus is on determining the stress intensity factor (SIF) as the key fracture parameter for evaluating the strength of the damaged material. The damaged plate is subjected to a uniform tensile stress of 1 MPa, and due to its small dimensions, the assumption of plane stress conditions is applied. To optimize the selected model, the normalized stress intensity factor (NSIF) is calculated as the ratio between the repaired and unrepaired plate, adjusted by subtracting the tensile load value. This is expressed by the formula:

$$NSIF = \sigma_p - \frac{K_P}{K} \tag{6}$$

Where:

- K_P is the Patched Stress Intensity Factor (for the repaired plate)
- K represents the SIF for the damaged (unrepaired) plate
- σ_p is the applied load.

5.3. Effect of crack length

The present study aimed to investigate the efficacy of bonded patches in mitigating the detrimental effects of cracks in aircraft plate structures. To achieve this, a series of numerical simulations were conducted on plates with varying crack lengths, ranging from 5 mm to 15 mm, as depicted in Fig. 10. The primary metric used to evaluate the effectiveness of the patch was the normalized SIF, which represents the ratio of the SIF in the repaired plate to that of the unrepaired plate under uniaxial loading.

The analysis revealed a clear trend: as the crack length increased, the normalized SIF decreased. This observation underscores the significant benefit of employing fiber-reinforced composite patches for repairing longer cracks. The composite material's inherent strength and ability to distribute stresses effectively contribute to a marked reduction in the likelihood of crack propagation. Consequently, the findings suggest that bonded composite patches are a highly promising approach for enhancing the structural integrity of aircraft plates, particularly in cases where cracks have progressed to substantial lengths.

5.4. Effect of adhesive thickness

Fig. 11 shows the relationship between the normalized SIF and adhesive thickness in a bonded composite repair system. The normalized SIF is plotted on the vertical axis, while the adhesive thickness in millimeters (mm) is plotted on the horizontal axis. As the adhesive thickness increases from 0.025 mm to 0.035 mm, the normalized SIF also increases, as indicated by the upward slope of the line.

This trend suggests that thicker adhesive layer's lead to higher

Table 8
SIF comparison between simulation and experiment (in MPa $\sqrt{m}$).

Case	Simulation	Experiment	Percentage of error (%)
Unrepaired specimen	0.11055	0.11695	5.465
Repaired specimen	0.05788	0.06238	7.214

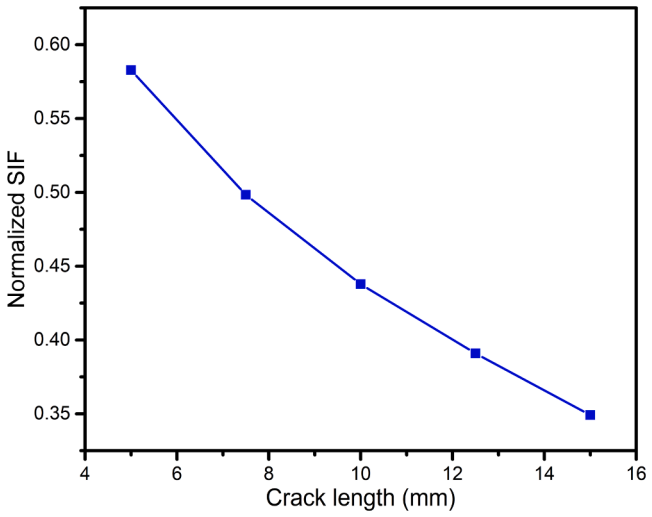

Fig. 10. Effect of crack length.

normalized SIF values in the repaired system. In the context of bonded composite repairs, the adhesive layer plays a critical role in transferring load between the cracked substrate and the repair patch. An increase in adhesive thickness can enhance the distribution of stresses around the crack tip, thereby affecting the repair performance. However, the relationship between adhesive thickness and SIF is not always linear in real-world applications. Beyond a certain thickness, adhesive performance can degrade due to factors like increased shear stresses within the adhesive layer or failure modes such as adhesive peeling or debonding. Therefore, while the figure demonstrates a direct increase in normalized SIF with adhesive thickness, it is important to investigate whether this trend continues for thicker adhesives or if a threshold exists where performance begins to decline. Overall, this figure highlights that optimizing the adhesive thickness is critical to achieving efficient crack repair. It emphasizes that while thicker adhesives may provide better load transfer initially, the design must balance adhesive properties with the mechanical performance of the composite repair system for optimal repair efficiency. Further experimental or simulation work might be needed to assess whether this trend holds for a wider range of thicknesses.

5.5. Effect of patch dimension

When examining the effect of patch thickness on the normalized SIF (Fig. 12a), it has been observed a clear trend: as the thickness of the patch increases, the normalized SIF decreases. This relationship means that a thicker patch helps reduce the concentration of stress around the crack area. A thicker patch can carry and distribute more load, which prevents stress from building up directly at the crack. This finding highlights that patch thickness is a significant factor in strengthening the repair because it enhances the ability of the patch to transfer loads smoothly over the cracked area. However, while adding thickness generally improves the repair, there is a need to avoid making the patch too stiff. Excessive stiffness could cause stress to concentrate around the patch edges instead, potentially leading to debonding or failure at these points. Therefore, optimal thickness helps to lower the SIF without introducing new stress issues at the edges of the patch.

Interestingly, when conducted the simulations on the effect of increasing patch height (Fig. 12b), it has been found the opposite effect with thickness. As patch height increases, normalized SIF also increases. This trend suggests that increasing patch height does not improve stress distribution and can make the repair less effective. The reason for this is that as patch height grows, the rigidity across the patch becomes uneven, with some areas becoming too stiff while others remain unsupported. This difference creates localized stress concentrations near the edges of the patch, where the patch transitions to the plate. Although a taller patch covers a larger portion of the damaged adhesive area, it does not necessarily help in reinforcing the repair. Instead, stress around the edges can rise due to uneven load transfer, which increases SIF. To achieve an effective repair, it is better to keep the patch height moderate. This way, the patch covers the damage but does not create high rigidity differences that increase stress near the crack.

The results for patch width (Fig. 12c) show a similar effect to thickness. When the width of the patch is increased, the normalized SIF decreases. This effect occurs because a wider patch helps to spread out the stress over a broader area, which prevents it from concentrating around the crack. However, we also observed that there is a practical limit to increasing patch width. Making the patch much wider than twice the crack length does not continue to provide a significant reduction in SIF and uses more material than necessary. Therefore, an ideal patch width is around twice the crack length, as it provides a balanced reduction in SIF without excessive material use or added weight.

These results indicate that patch thickness, height, and width play different roles in reducing stress around the crack. A thicker patch is beneficial as it reduces the SIF by distributing stress more evenly across the repair area, strengthening the repair overall. Similarly, a wider patch also helps reduce the SIF, as it spreads the stress over a larger area. However, when it comes to patch height, increasing it too much has a negative effect, raising the SIF and potentially weakening the repair. This occurs because excess height causes stiffness to become uneven, creating higher stress near the unsupported areas of the patch.

5.6. Optimization results

This article also observed the parametric effects using the DOE method for a defined problem stated in Fig. 7. The ANOVA (analysis of variance) is one of the common approaches to investigate the effect of each parameter in the DOE method. Hence, considered an ANOVA Table as the first observation of this study (Table 9). A 3 level L_9 orthogonal array of 4 parameters with nine simulations run was determined in this analysis. The total DF for the simulation is 8 $(= 9 - 1)$ in an

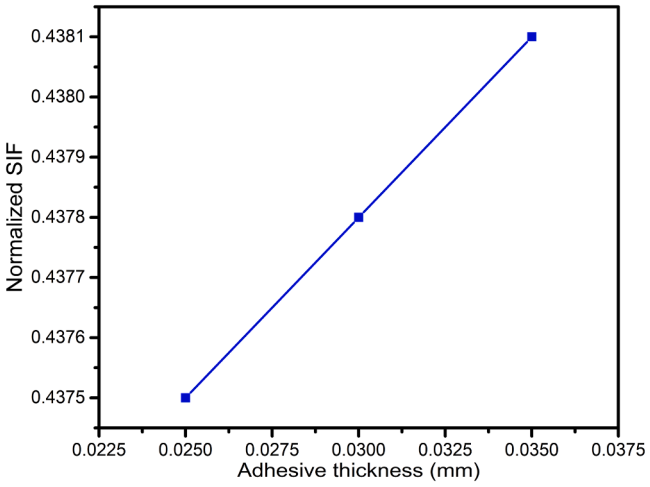

Fig. 11. Effect of adhesive thickness.

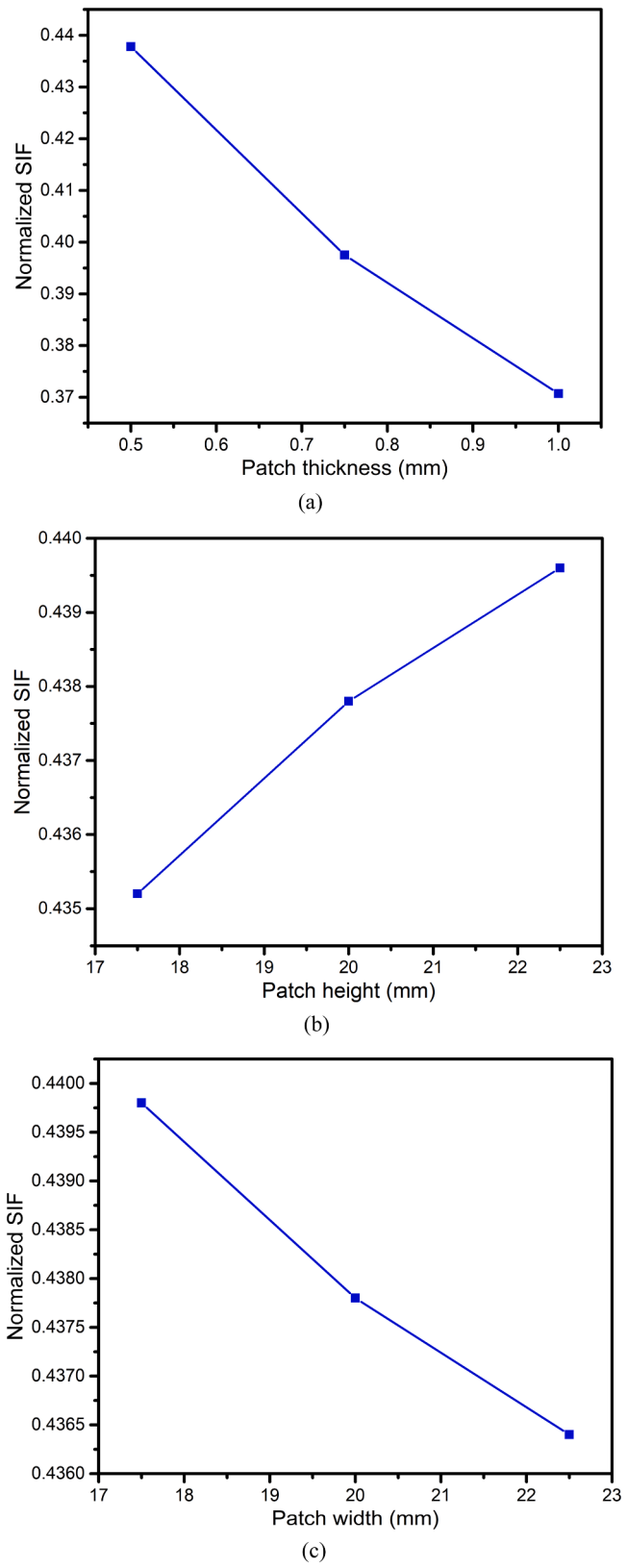

Fig. 12. Effect of composite patch (a) thickness (b) height (c) width.

Table 9
ANOVA Table.

Source	DF	Adj SS	Adj MS	F-Value	P-Value
Regression	5	0.000484	0.000097	1.54	0.384
Tp	1	0.000054	0.000054	0.86	0.421
Wp	1	0.000142	0.000142	2.25	0.230
Hp	1	0.000079	0.000079	1.26	0.343
M	2	0.000218	0.000109	1.73	0.316
Error	3	0.000189	0.000063		
Total	8	0.000672			

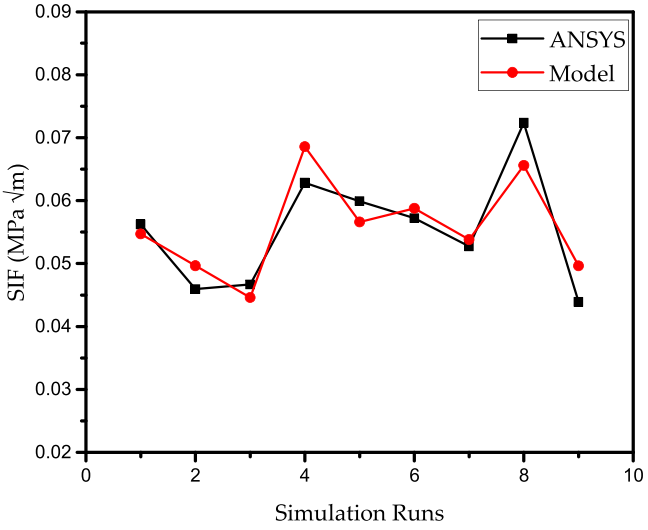

Fig. 13. Comparison between the simulation result of SIF and those obtained by the regression equation.

ANOVA Table. Table 9 shows the effect of each parameter on the value of SIF with its desired specific value from each column. As per the ANOVA analysis, it has been observed that the DF of each parameter assigned 1 with the error value of DF is 3. Hence, the interpretation of the ANOVA Table with the test statistic is the *F*-value of 1.54 and the obtained *P*-value of 1.54 is 0.384 is less than to the level of significance (α), the null hypothesis gets rejected and concludes that there is a (statistically) significant difference among the regression means. Similarly, for the other parameters have the same conclusion that some of the Tp, Wp, and Hp have different means. Therefore, as per the present results of SIF, the value is always varied with the level of each parameter.

For the function of thickness, width, and height, a linear polynomial model shown below, which represents the SIF of each composite material type. The regression equation is as given below.

Regression Equation,

1. Glass/Epoxy (GE)

$$SIF = 0.0648 - 0.0123\ Tp - 0.001123\ Wp + 0.000728\ Hp \quad (7)$$

2. Carbon/Epoxy (CE)

$$SIF = 0.0770 - 0.0123\ Tp - 0.001123\ Wp + 0.000728\ Hp \quad (8)$$

3. Boron/Epoxy (BE)

$$SIF = 0.0715 - 0.0123Tp - 0.001123\ Wp + 0.000728\ Hp \quad (9)$$

Fig. 13 compares the values of the SIF's which is obtained by the FE method with those calculated from the regression equations of each material type. Comprehensively, the model's curve and the numerical data demonstrate a strong degree of agreement. But, for some of the case of 4, 5, 8, and 9 the model shows a slight variation in results because of the changes in material type means that the material has large variation when it combined with the patch dimensions. This is because each

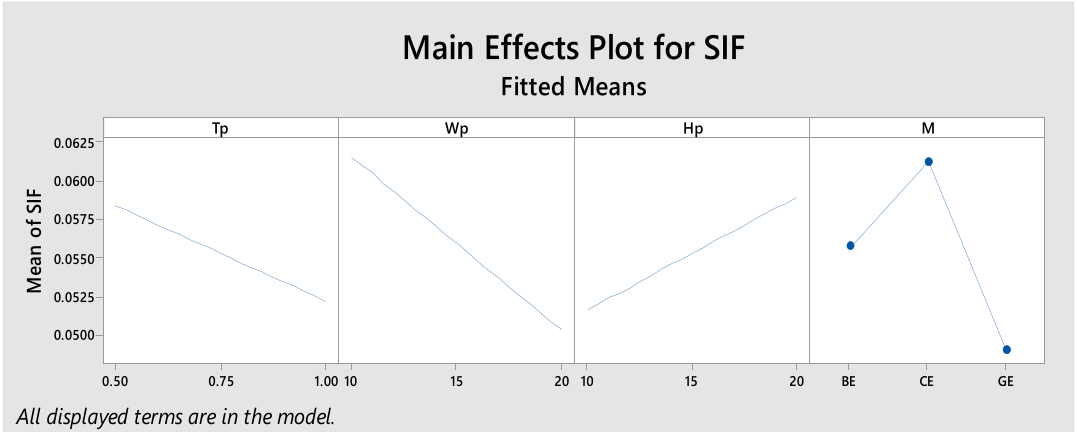

(a)

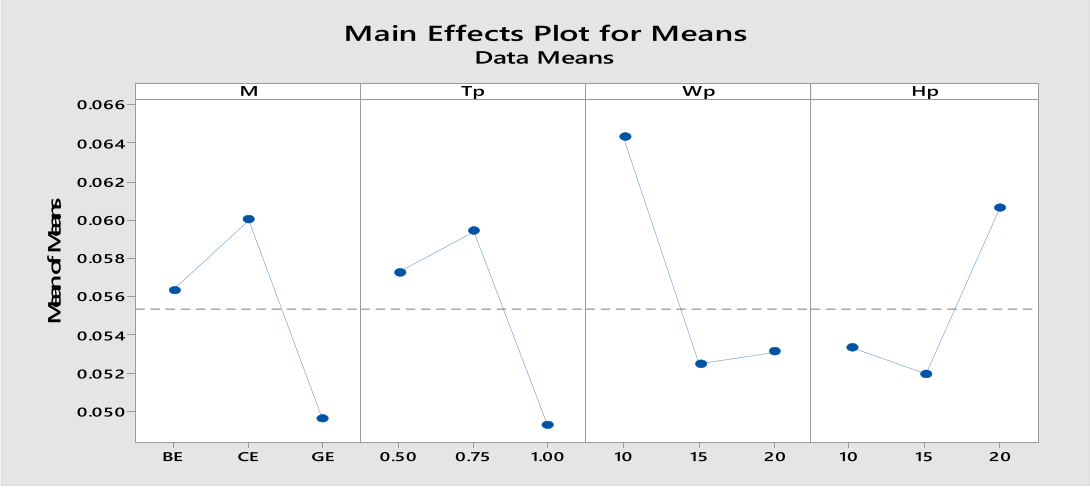

(b)

Fig. 14. Main effect Plots (a) for SIF (b) for Means.

material has different mechanical properties which in results the model can give different results when compared with numerical values. This linear regression equation allows us to obtain an accurate prediction of SIF.

Upon comparing the results of the simulation and regression analysis, a deviation pattern was observed. This variance is due to the simplified assumptions inherent in the regression model, which approximates the relationship between patch parameters and SIF based on linear relationships. In contrast, the FE simulation accounts for detailed interactions within the patch and plate, including complex stress distributions near the crack and patch edges. These differences result in slight deviations, particularly in cases where high patch thickness and width contribute to non-linear stress responses. Despite these deviations, the regression model provides a reliable approximation of the overall trends, allowing us to predict SIF changes effectively for various patch configurations.

In this study, we observed the main effect plot from the selected parameters in two different forms which are shown in Fig. 14. In both plots, the variation is completely different one case shows the main effect plot of SIF other is means. According to Fig. 14(a), continuous factors such as patch thickness, width, and height show the different variations in SIF reduction. But the thickness and width performance shown higher in ranges will result in a reduction of SIF whereas the height of the patch shows opposite to this. These variations are categorized with the composite material type and in this, the glass/epoxy shows influenced more on the reduction of SIF with these parameter combinations.

Fig. 14(b) illustrates the mean value of SIF from each level of the parameter for the average ratio of SIF. Each parameter has a different variation which is increasing/decreasing. For the case patch material at a lower level, the value of SIF is low followed by level two the SIF increases then decreases at a higher level. This shows when patch material is combined with other parameters how it affects the SIF value due to the interaction with other parameters. Similarly, for the case of thickness, width, and height of the patch it behaves differently with their levels due to interaction with each other. This study shows the effects of each parameter on their levels.

To determine whether the present model is adequate and meets the assumption of the analysis; residual plots for SIF have been obtained from the software shown in Fig. 15.

The normal probability plot of residuals is used to check the assumption that residuals follow a normal distribution. Ideally, the points on this plot should form a straight line. However, deviations from this pattern can indicate potential issues with the model: a non-linear pattern suggests non-normality, an outlying point indicates an outlier, and a changing slope might point to an unaccounted variable. Additionally, the residuals versus order plot helps confirm whether the residuals are independent. Independent residuals should not display any discernible patterns when plotted in time order. Any visible patterns may suggest correlation among nearby residuals, indicating a lack of independence. Ideally, residuals should appear randomly distributed around the centerline in this plot.

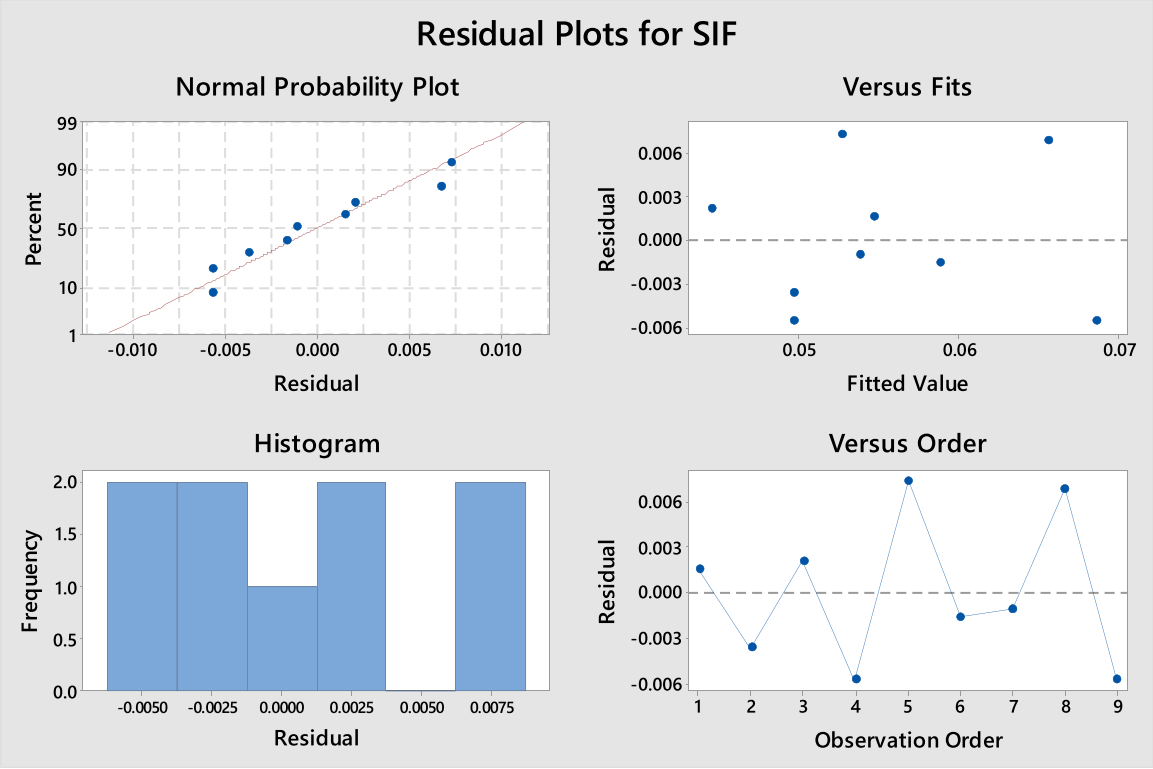

Fig. 15. Residual Plots for SIF.

In a residual versus fits plot, positive residuals on the y-axis imply that the prediction was too low, while negative values indicate the prediction was too high, with zero meaning an exact prediction. If the points are not evenly distributed vertically, or if there is an outlier or a clear shape, it may suggest issues with the model. Overall, the residuals versus fits plot are used to check if the residuals are randomly distributed with constant variance. In this specific case, the residuals on the normal probability plot generally follow a straight line. From the residuals versus fits plot, it is observed that there are six observations in each of the four groups. Given that this design does not meet the sample size guidelines, satisfying the normality assumption is crucial for the reliability of the test results.

Fig. 16 shows the contour plot of the results from this optimization. In this graph, darker regions of the blue colors indicate the lowest SIF. The plots have been categorized for each materials type Fig. 16(a) represents the contour results for glass/epoxy composite materials patch in which the lowest value of SIF has been found <0.042 MPa$\sqrt{\text{m}}$ when the thickness and width have in highest range and *Hp* at a higher level and *Wp* at a lower level. This value of SIF also the highest reduction of this contours observation as compared to the other type of materials. When the type of the material is carbon/epoxy and boron/epoxy it has been found that the reduction of SIF found like the combinations of the parameter of glass/epoxy with the value of SIF 0.0550 MPa$\sqrt{\text{m}}$ and 0.050 MPa$\sqrt{\text{m}}$ respectively.

Moreover, the increase of composite patch thickness will result in a decrease of SIF in each composite material type. Whereas the height and width of the composite patch depend on the combined parameters. From the present L_9 orthogonal array the glass/epoxy materials shown the leading influence in reducing the highest value of SIF of the present form. Therefore, this may be different when the selection of materials type is not the same as in the present form.

To achieve the best results, a response optimization analysis was conducted, with the findings presented in Table 10 and Fig. 17. The analysis predicts the lowest possible SIF value at 0.0365244 MPa$\sqrt{\text{m}}$, but this is impractical because the shear stress on the adhesive surface would be excessively high, potentially causing failure. A more realistic and safe SIF value is around 0.0373007 MPa$\sqrt{\text{m}}$, which can be obtained using a composite material of glass/epoxy, with a composite patch thickness of 1 mm, a width of 20 mm, and a height of 10 mm. Finite Element Analysis (FEA) was performed using these parameters, yielding an SIF of 0.038127 MPa$\sqrt{\text{m}}$, which is very close to the optimal value predicted by the optimization study.

6. Conclusion

By analyzing the results, it is evident that the efficiency of repairing cracked aluminum plates can be significantly improved by optimizing key factors such as patch dimensions, adhesive thickness, and crack length. The study demonstrated that the SIF generally decreases with an increase in these parameters, except for patch height, where an increase leads to a rise in SIF. The experimental results closely align with numerical simulations, showing a discrepancy of only 6 to 8 percent, validating the accuracy of the adopted methods. The scientific novelty of this work lies in the combined experimental and numerical approach that employs a design of experiments methodology to identify the optimum repair configurations. This approach not only ensures energy savings and cost efficiency but also proves essential in guiding practical applications. Optimizing the data before conducting parametric observations further emphasizes the importance of precision in repair strategies. Despite its strengths, certain limitations were identified, such as

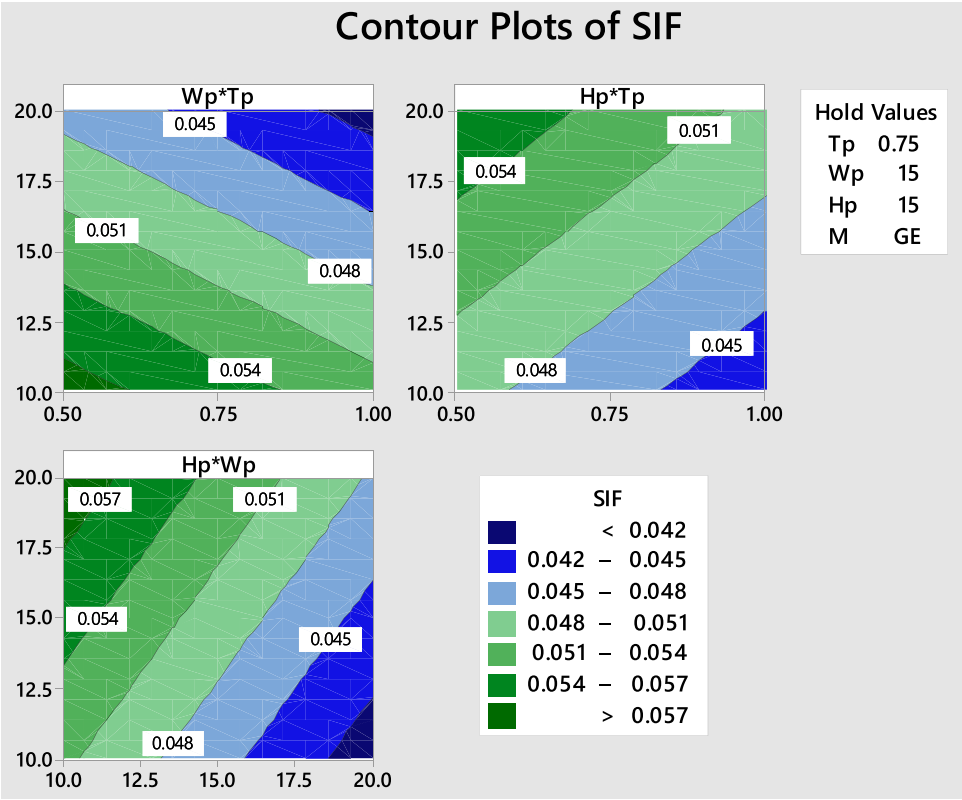

(a)

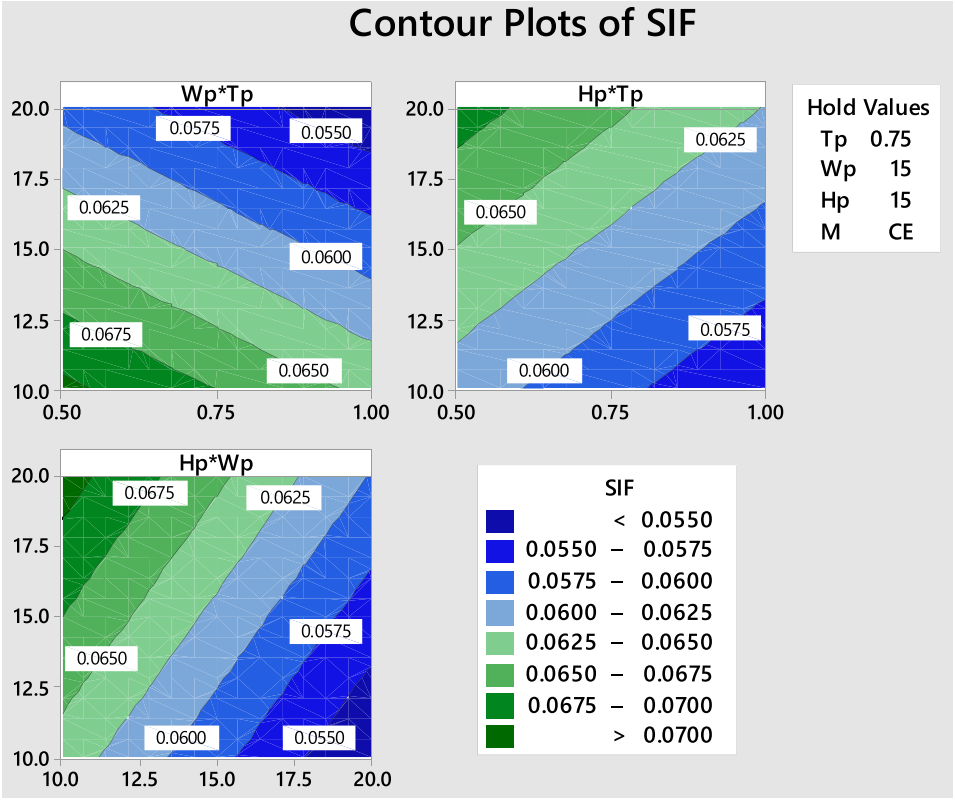

(b)

Fig. 16. Contours result of each material type (a) Glass/Epoxy (b) Carbon/Epoxy (c) Boron/Epoxy.

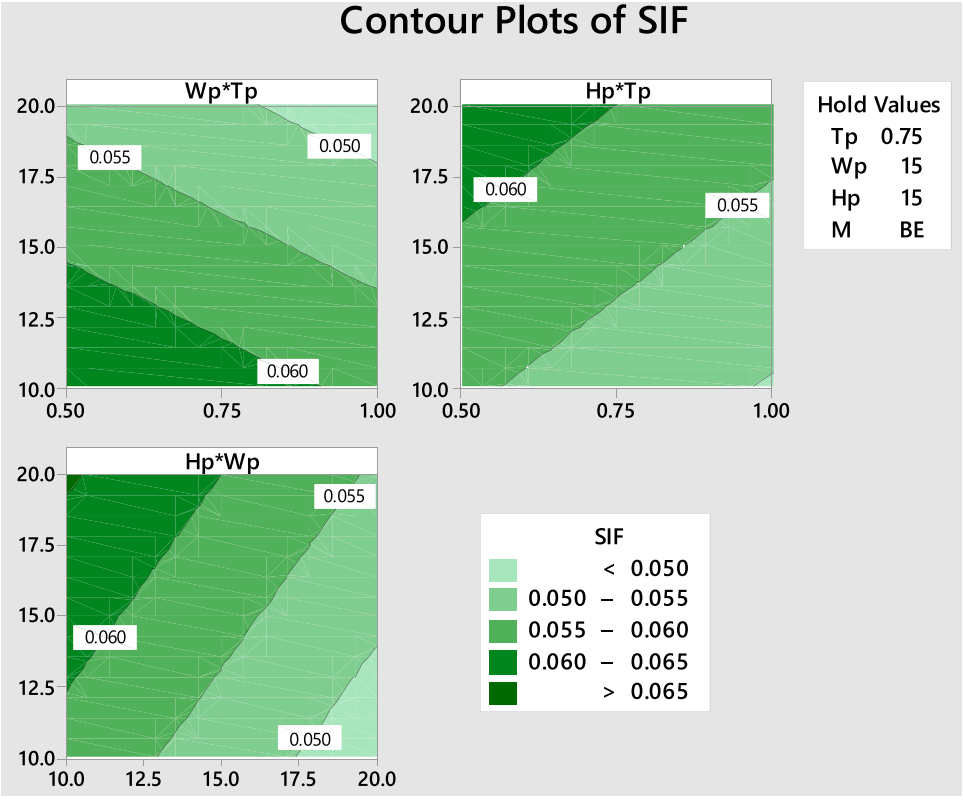

(c)

Fig. 16. (*continued*).

Table 10
SIF optimization prediction.

Response	Goal	Lower	Target	Upper	Weight	Importance
SIF	Minimum	0.0365244	0.043916	0.072376	1	1
Solution	**M**	**Tp**	**Wp**	**Hp**	**SIF (K) Fit**	**Composite Desirability**
1	GE	1	20	10	0.0373007	1

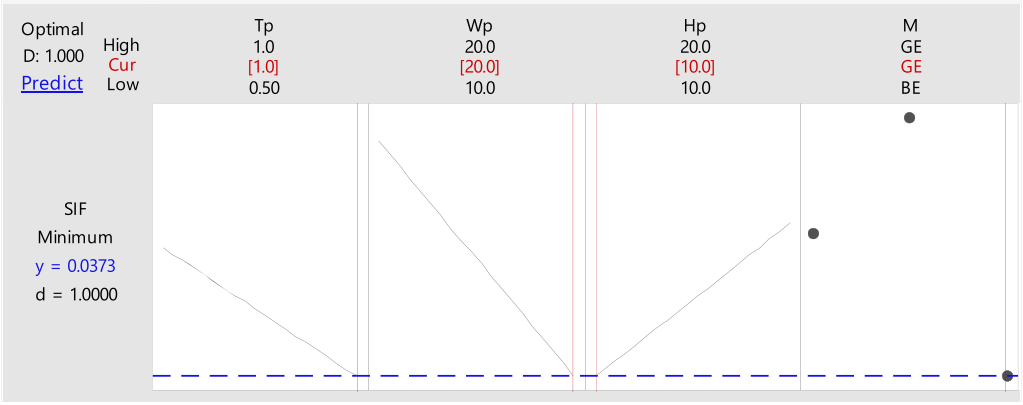

Fig. 17. Prediction plot.

the impact of adhesive thickness on repair efficiency and the challenges in accurately modeling complex stress distributions at the interface. Addressing these limitations in future studies could further enhance the applicability of this method. Future work should explore the durability of these repairs under various operational conditions, including cyclic loading and environmental factors, while integrating advanced predictive modeling techniques. Also, the findings have potential applications in extending the service life of cracked components and can also be applied across industries such as automotive, marine, and civil engineering.

CRediT authorship contribution statement

Abdul Aabid: Writing – original draft, Methodology, Investigation, Formal analysis, Conceptualization. **Muhammad Nur Syafiq Bin Rosli:** Methodology, Investigation, Conceptualization. **Meftah Hrairi:** Writing – review & editing, Supervision, Formal analysis. **Muneer Baig:** Funding acquisition, Formal analysis, Data curation.

Declaration of competing interest

The authors declare that they have no known competing financial interests or personal relationships that could have appeared to influence the work reported in this paper.

Acknowledgement

This research was supported by the Ministry of Education of Malaysia (MOE) through the Fundamental Research Grant Scheme (FRGS/1/2021/TK0/UIAM/01/5). Furthermore, the authors acknowledge the support of the Structures and Materials (S&M) Research Lab of Prince Sultan University and Prince Sultan University for paying this publication's article processing charges (APC).

Data availability

Data will be made available on request.

References

[1] A. Aabid, M. Baig, M. Hrairi, J. Syed, M. Ali, Effect of fiber orientation-based composite lamina on mitigation of stress intensity factor for a repaired plate: a finite element study, Frattura Ed Integrità Strutturale 68 (2024) 209–221, https://doi.org/10.3221/IGF-ESIS.69.14.

[2] A. Aabid, M. Hrairi, J.S.M. Ali, Optimization of composite patch repair for center-cracked rectangular plate using design of experiments method, Mater. Today 27 (Part 2) (2020) 1713–1719, https://doi.org/10.1016/j.matpr.2020.03.639.

[3] A. Aabid, M. Hrairi, J.S.M. Ali, A. Abuzaid, Numerical analysis of cracks emanating from hole in plate repaired by composite patch, Int. J. Mech. Prod. Eng. Res. Develop. (IJMPERD) 4 (8) (2018) 238–243.

[4] A. Aabid, M. Hrairi, J.S.M. Ali, A. Abuzaid, Effect of bonded composite patch on the stress intensity factors for a center-cracked plate, IIUM Eng. Journal 20 (2) (2019) 211–221.

[5] A. Aabid, M. Hrairi, J.S.M. Ali, A. Abuzaid, Effect of bonded composite patch on the stress intensity factor for a center-cracked plate, IIUM Eng. J. (2019), https://doi.org/10.31436/iiumej.v20i2.912.

[6] A. Aabid, M.A. Raheman, M. Hrairi, M. Baig, Improving the performance of damage repair in thin-walled structures with analytical data and machine learning algorithms, Frattura Ed Integrità Strutturale 68 (2024) 310–324, https://doi.org/10.3221/IGF-ESIS.68.21.

[7] A. Abuzaid, M. Hrairi, M.S. Dawood, Experimental and numerical analysis of piezoelectric active repair of edge-cracked plate, J. Intell. Mater. Syst. Struct. 29 (18) (2018) 3656–3666, https://doi.org/10.1177/1045389×18798949.

[8] H.A. Aglan, Y.X. Gan, Q.Y. Wang, M. Kehoe, Design guidelines for composite patches bonded to cracked aluminum substrates, J. Adhes. Sci. Technol. 16 (2) (2002) 197–211, https://doi.org/10.1163/156856102317293704.

[9] A.A. Baker, Repair efficiency in fatigue-cracked aluminium components reinforced with boron/epoxy patches, Fatigue Fract. Eng. Mater. Struct. 16 (7) (1993) 753–765, https://doi.org/10.1111/j.1460-2695.1993.tb00117.x.

[10] M.D. Banea, L.F.M. Da Silva, Adhesively bonded joints in composite materials: an overview, Proceed. Inst. Mech. Eng., Part L. 223 (1) (2009) 1–18, https://doi.org/10.1243/14644207JMDA219.

[11] M. Belhouari, S.M. Fekih, K. Madani, A. Amiri, B.A. Bachir Bouiadjra, Experiments method design applied to optimization of patch repairs for cracked plates, Key Eng. Mater. 577–578 (2013) 441–444, https://doi.org/10.4028/www.scientific.net/kem.577-578.441.

[12] A. Belhoucine, K. Madani, Effect of the composite patch beveling on the reduction of stresses in 2024-T3 Aluminum structure damaged and repaired by composite, hybrid patch repair, Struct. Eng. Mech. 82 (1) (2022) 17–30.

[13] C. Chen, T. Hai Tran, A.A. Volinsky, Bonded composite repair structures multiple site damage analysis, Aircraft Eng. Aerospace Techn. 85 (3) (2013) 171–177, https://doi.org/10.1108/00022661311313560.

[14] J. Cheng, F. Taheri, H. Han, Strength improvement of a smart adhesive bonded joint system by partially integrated piezoelectric patches, J. Adhes. Sci. Technol. 20 (6) (2006) 503–518, https://doi.org/10.1163/156856106777213285.

[15] S.C. Djebbar, N. Kaddouri, M. Elajrami, M. Belhouari, K. Madani, Use of combined CZM and XFEM techniques for the patch shape performance analysis on the behavior of a 2024-T3 Aluminum structure reinforced with a composite patch, Frattura Ed Integrita Strutturale 16 (62) (2022) 304–325, https://doi.org/10.3221/IGF-ESIS.62.22.

[16] S.M. Fekih, A. Albedah, F. Benyahia, M. Belhouari, B.B. Bouiadjra, A. Miloudi, Optimisation of the sizes of bonded composite repair in aircraft structures, Mater. Des. 41 (2012) 171–176, https://doi.org/10.1016/j.matdes.2012.04.025.

[17] S.C. Her, S.J. Liu, Load transfer in adhesive double-sided patch joints, J. Adhes. Sci. Technol. 28 (14–15) (2014) 1517–1529, https://doi.org/10.1080/01694243.2012.698123.

[18] N. Kaddouri, K. Madani, L. Rezgani, M. Mokhtari, X. Feaugas, Analysis of the effect of modifying the thickness of a damaged and repaired plate by composite patch on the J-Integral; effect of bonding defects, J. Bra. Soc. Mech. Sci. Eng. 42 (8) (2020) 426, https://doi.org/10.1007/s40430-020-02515-y.

[19] M.R. Kalestan, H.M. Kashani, A.P. Anaraki, F.A. Ghasemi, Experimental and num erical investigation of fatigue crack growth in aluminum plates repaired by FML composite patch, Int. J. Struct. Integr. 5 (4) (2014) 242–252, https://doi.org/10.1108/IJSI-08-2013-0019.

[20] K. Madani, S. Touzain, X. Feaugas, M. Benguediab, M. Ratwani, Stress distribution in a 2024-T3 aluminum plate with a circular notch, repaired by a graphite/epoxy composite patch, Int. J. Adhes. Adhes. 29 (3) (2009) 225–233, https://doi.org/10.1016/J.IJADHADH.2008.05.004.

[21] Montgomery, D.C. (2012). Design and Analysis of Experiments.

[22] R.D.F. Moreira, R.D.S.G Campilho, Strength improvement of adhesively-bonded scarf repairs in aluminium structures with external reinforcements, Eng. Struct. 101 (2015) 99–110, https://doi.org/10.1016/j.engstruct.2015.07.001.

[23] W. Oudad, B.B. Bouiadjra, M. Belhouari, S. Touzain, X. Feaugas, Analysis of the plastic zone size ahead of repaired cracks with bonded composite patch of metallic aircraft structures, Comput. Mater. Sci. 46 (4) (2009) 950–954, https://doi.org/10.1016/j.commatsci.2009.04.041.

[24] G.A. Papadopoulos, B. Badalouka, J. Souyiannis, Experimental study of the reduction at crack-tip stress intensity factor K_I by bonded patch, Int. J. Fract. 149 (2) (2008) 199–205, https://doi.org/10.1007/s10704-008-9240-4.

[25] M. Ratwani, Analysis of cracked, adhesively bonded laminated structures, AIAA J. 17 (9) (1979) 988–994, https://doi.org/10.2514/3.61263.

[26] F. Ricci, F. Franco, N. Monrefusco, Bonded composite patch repairs on cracked aluminum plates: theory, modeling and experiments. Advances in Composite Materials - Ecodesign and Analysis, 2011, pp. 445–464, https://doi.org/10.5772/16227.

[27] R. Ružek, R. Doubrava, J. Raška, Wing repair using an adhesively bonded boron composite patch - Design and verification, Int. J. Struct. Integr. 6 (2) (2015) 259–278, https://doi.org/10.1108/IJSI-10-2013-0027.

[28] K. Saeed, M. Abid, Crack growth performance of aluminum plates repaired with composite and metallic patches under fatigue loading, in: ICASE 2015 - 4th International conference on aerospace science and engineering, 2016, https://doi.org/10.1109/ICASE.2015.7489504.

[29] H. Sarangi, K.S.R.K. Murthy, D. Chakraborty, Radial locations of strain gages for accurate measurement of mode I stress intensity factor, Mater. Des. 31 (6) (2010) 2840–2850, https://doi.org/10.1016/j.matdes.2009.12.043.

[30] Sato, M., Yokobori, A.T., & Ozawa, Y. (2002). Experimental study of repair efficiency for single-sided. 11(1), 51–59.

[31] N.H. Sebaibi, R. Mhamdia, K. Madani, N. Kaddouri, S.C.H. Djabbar, R.D.S. G. Campilho, Analysis of the performance of carbon fiber patches on improving the failure strength of a damaged and repaired plate, J. Braz. Soc. Mech. Sci. Eng. 46 (6) (2024) 347, https://doi.org/10.1007/s40430-024-04881-3.

[32] Y. Shibuya, S. Fujimoto, D. Aoki, M. Sato, H. Shirahata, H. Fukunaga, H. Sekine, Evaluation of crack growth in cracked aluminum panels repaired with a bonded composite patch under cyclic loading, Adv.Compos. Mater. 10 (4) (2001) 287–297, https://doi.org/10.1163/156855101753415319.

[33] A.A. Yala, N. Demouche, S. Beddek, K. Hamid, Full analysis of all composite patch repairing design parameters, Iran. J. Mater. Sci. Eng. 15 (4) (2018) 70–77, https://doi.org/10.22068/ijmse.15.4.70.

[34] A.A. Yala, A. Megueni, Optimisation of composite patches repairs with the design of experiments method, Mater. Des. 30 (2009) 200–205, https://doi.org/10.1016/j.matdes.2008.04.049.